Kinetics of 2-Hexanol and 3-Hexanol Oxidation Reaction over TS-1 Catalysts

J. E. Gallot, M. P. Kapoor, and S. Kaliaguine
Dépt. de Génie chimique, Université Laval, Ste Foy, Québec (Québec), G1K 7P4 Canada

A kinetic investigation of the catalytic oxidation of 2-(3-) hexanols to 2-(3-) hexanones over a series of titanium silicalites [TS-1] is reported. This study considers the biphasic character of the reaction medium and uses the mathematical theory of linear graphs to derive rate equations for both hexanols' oxidation and hydrogen peroxide's decomposition. The 2-hexanols' oxidation is usually considered as the secondary reaction in the n-hexane oxyfunctionalization process. Comparing the kinetic constants obtained in this study and those generated by the analysis of previously published n-hexane oxyfunctionalization rate data allows one to conclude that in the latter case, hexanones are also produced by a direct primary oxidation of n-hexane.

Introduction

To overcome the basic environmental problems arising from the industrial use of homogeneous catalysts and with the aim of developing friendly environmentally "clean" oxidation processes, the use of solid catalysts such as titanium silicalites (TS) with diluted hydrogen peroxide as the oxidizing agent is of current interest. The observation of the remarkable activity of TS-1 (of MFI structure) in numerous oxidation reactions (Clerici, 1991; Esposito et al., 1985; Huybrechts et al., 1990; Roffia and Padovan, 1987; Tatsumi et al., 1990) is therefore attracting much attention, as it opens the way to its wide application in the field of fine chemicals synthesis.

Since the discovery of the catalytic effect of these TS materials, several studies dealing with the identification of the titanium active site in TS have been conducted (Boccuti et al., 1989; Behrens et al., 1991; Bellussi et al., 1992; Deo et al., 1993; LeNoc et al., 1995; Perego et al., 1986; Trong On et al., 1992a,b; Tuel et al., 1990). It was reported that framework titanium species are directly involved in the catalytic activation of the relatively inert carbon–hydrogen bond of alkanes (Huybrechts et al., 1992; Millini et al., 1992; Uguina et al., 1995).

However, only a limited number of studies have focused so far on the mechanism and the kinetics of the *n*-hexane oxyfunctionalization reactions on titanium silicalites and using diluted hydrogen peroxide. One possible reason for this situation is that this oxidation process is actually conducted in a multiphase reaction medium (liquid–liquid–solid) with a complex parallel-consecutive reaction scheme. Our previous investigations of this reaction network were aiming at an analysis of the solvent effects on reaction rates (Gallot et al., 1996) and a correlation between the kinetic parameters and the state and content of Ti in these catalysts (Gallot et al., 1997).

Although the *n*-hexane oxyfunctionalization products involve a mixture of the isomers 2- and 3-hexanol, 2- and 3-hexanone, our previous kinetic analysis was performed using the following lumped stoichiometric reaction scheme:

$$\begin{array}{l} H_2O_2 + C_6H_{14} \xrightarrow{(1)} C_6H_{14}O + H_2O \xrightarrow[H_2O_2]{(2)} C_6H_{12}O + 2H_2O \\ \quad\Big| \xrightarrow{(3)} H_2O + 1/2\,O_2\,(g), \end{array} \qquad (1)$$

where $C_6H_{14}O$ and $C_6H_{12}O$ are pseudocomponents used, respectively, for hexanol isomers and the corresponding hexanone isomers. It was pointed out, however, that the selectivity of hexanones formation still has a nonzero value when the *n*-hexane conversion tends to zero (Gallot et al., 1997). Such a result is not consistent with the preceding scheme.

The objectives of the present study were therefore to reexamine the reaction network of *n*-hexane oxyfunctionalization by a more detailed kinetic analysis. The methodology developed in our new approach was to first deal with the kinetic investigation of the catalytic oxidation of 2- and 3-hexanol on

Correspondence concerning this article should be addressed to S. Kaliaguine.

TS-1. Another point that needs clarification stems from the report by van der Pol and van Hoof (1993) that the oxidation rate of 2-octanol was first order with respect to H_2O_2 and zero order with respect to the alcohol. This is indeed in contrast with the kinetics employed in our modeling of *n*-hexane oxyfunctionalization, in which the hexanol oxidation to hexanone (Reaction 2) was considered of second order with respect to H_2O_2 and of first order with respect to the alcohol.

Another objective of the present article is to compare the kinetic parameters established from 2,3-hexanol oxidation data with the values adopted previously for the same parameters in the treatment of *n*-hexane oxyfunctionalization kinetic data.

Experimental Studies

Catalyst preparation

Six TS-1 samples with Ti/(Ti+Si) atomic ratios varying from 0.010 to 0.060 were synthesized hydrothermally. The gel was prepared from an appropriate mixture of tetraethylorthosilicate (TEOS), tetraethylorthotitanate (TEOT), and sodium-free tetrapropyl ammonium hydroxide (TPAOH) in propanol as organic template. The hydrothermal crystallization was performed in a Teflon-lined stainless steel autoclave at 175°C for 96 h. The solid was then filtered, washed, dried, and calcined at 550°C.

The physicochemical characterization results (AA, XRD, FTIR, UV-visible spectroscopy, XANES, EXAFS, SEM) of this series of TS-1 samples have been the object of discussion in previous works (Gallot et al., 1997; Cartier et al., 1995). It has been reported that samples synthesized with titanium contents lower than 1.9% Ti/(Ti+Si) have a UV-visible single band at about 200–220 nm, which was assigned to isolated framework tetrahedral titanium. The band intensity was also found to be proportional to the titanium content. However, samples with higher titanium content (> 1.9%) showed a second band at about 280–330 nm, due to octahedral extraframework titanium species. Results from scanning electron microscopy revealed homogeneous TS-1 particles with an average particle size smaller than 0.12 μm.

Catalytic reactions

The oxidation of *n*-hexane and 2- (3-) hexanol were performed in a 180-mL glass reactor equipped with a constant-temperature water bath, a reflux condenser, and a gas collector. Dilute aqueous H_2O_2 (30 wt. %) was used as the oxidant and methanol as the solvent. In a typical reaction, 250 mg of the catalyst, 0.1163 mol of *n*-hexane, 5 g of methanol, and 0.0441 mol of hydrogen peroxide were used in the oxidation of *n*-hexane. For the oxidation of hexanols, 125 mg of catalyst, 0.0476 mol of hexanols, 0–7.75 g of methanol as solvent, and 0.02205 mol of H_2O_2 were used. The reactions were carried out at 45°C, 55°C, 60°C, 65°C, or 70°C (55°C for the *n*-hexane oxyfunctionalization) under vigorous agitation and otherwise similar conditions. Quick tests were performed to verify that reaction rates were not dependent on the stirrer rotation speed.

The reaction rate was followed by collecting small-volume (0.2 mL) aliquots of the organic phase at different reaction times. The reaction products were analyzed using a gas chromatograph (HP 5890) equipped with a capillary column (DB wax) and a flame ionization detector (FID). At the same time, the volume of oxygen collected was recorded. At the end of the reaction, the two liquid phases were separated and the aqueous phase was filtered. The concentration of unconverted H_2O_2 in the aqueous phase was determined by iodometric titration.

Results and Discussion

Oxidation of 2- (3-) hexanol

GC analysis shows that the only products, 2-hexanone or 3-hexanone, are formed from 2-hexanol and 3-hexanol, respectively, during the oxidation reaction. The catalytic oxidation of 2- (3-) hexanol over titanium silicalites will then be described by the following reactions:

$$\underset{(B)}{C_6H_{14}O} + \underset{(A)}{H_2O_2} \longrightarrow \underset{(D)}{C_6H_{12}O} + 2H_2O \quad (2)$$

$$H_2O_2 \longrightarrow H_2O + 1/2O_2\,(g). \quad (3)$$

Designating by X_1 and X_2 the partial conversions of H_2O_2 through Reactions 2 and 3, respectively, the instantaneous mole numbers of 2-(3-) hexanol, hydrogen peroxide, and 2-(3-) hexanone will be written as

$$N_B = N_{B0} - N_{A0} \cdot X_1 \quad (4)$$

$$N_A = N_{A0} \cdot (1 - X_1 - X_2) \quad (5)$$

$$N_D = N_{A0} \cdot X_1 \quad (6)$$

$$N_{O_2} = 0.5 * N_{A0} \cdot X_2. \quad (7)$$

The experimental values of X_1 and X_2 were calculated using Eqs. 6 and 7 and the carbon balance was then always verified within less than 5% relative error.

The selectivity of H_2O_2 is defined as

$$S = \frac{N_D}{N_{A0} - N_A} = \frac{X_1}{X_1 + X_2}. \quad (8)$$

Tables 1 and 2 report the catalytic oxidation results of 2-hexanol and 3-hexanol in the presence of a series of TS-1 with different Ti contents and using different amounts of methanol as solvent. The reactions were conducted at temperatures varying between 45°C and 65°C or 70°C. The catalytic activities are expressed in terms of H_2O_2 and hexanol conversions. Figures 1a and 1b illustrate typical trends of the measured organic concentration of 3-hexanol as a function of a modified reaction time $t' = t \cdot W\text{cat}/N_{A0}$ (h·kg/kmol). Using a mass balance of hexanol in a two-phase batch reactor system, the rate of hexanol oxidation will be expressed as

$$\frac{dX_1}{d(t \cdot W\text{cat}/N_{A0})} = R_{1,i}(K_i^*, k, C_A, C_i^{*,\text{aq}}), \quad (9)$$

with $R_{1,i}$ the oxidation rates; K_i^* the phase equilibrium partition coefficient of component (i); k the kinetic constants;

Table 1. Catalytic Oxidation of 2-Hexanol over TS-1 Catalysts*

Exp. No.	React. Time (h)	2-Hexanol Conv. (mol. %)	H_2O_2 Conv. (mol. %)	H_2O_2 Select. as Defined in Eq. 8 (mol. %)
1	1	0.60	5.70	23.6
	2	1.02	11.7	19.4
	3	1.23	16.9	16.3
	4	2.11	23.9	19.7
	5	2.25	28.6	17.6
2	1	1.24	18.4	15.1
	2	1.36	27.5	10.9
	3	1.95	40.6	10.6
	4	2.46	51.5	10.5
	5	2.71	61.4	9.78
3	1	1.46	14.8	21.9
	2	1.71	27.4	13.9
	3	2.02	40.8	11.1
	4	2.94	54.8	11.9
	5	3.46	63.9	12.0
4	1	1.61	28.7	12.7
	2	1.95	41.7	10.4
	3	2.43	56.2	6.7
	4	3.35	66.5	11.2
	5	3.96	74.5	11.8
5	1	1.52	22.2	15.2
	2	1.70	38.9	9.72
	3	2.33	52.7	9.86
	4	2.87	63.7	10.0
	5	3.21	72.4	9.88
6	1	0.45	6.41	15.3
	2	0.85	12.4	15.2
	3	1.00	17.1	12.9
	4	1.33	21.8	13.6
	5	1.84	27.3	15.0

*Reaction conditions: catalyst 125 mg; temperature #1–4, 45, 55, 60 and 65°C; #5–6: 55°C; Ti/(Ti+Si) #1–6: 2.4%; methanol #1–4: 2.02 g; #5: 1.25 g; #6: 4.0 g; 2-hexanol: 4.76×10^{-2} mol; H_2O_2: 2.20×10^{-2} mol.

and symbols C denote aqueous or organic phase concentrations (see notation section), i = 2-hexanol or 3-hexanol.

Thus hexanol oxidation rates expressed in number of moles converted per hour per kg of catalyst are proportional to the slopes of the curves in Figures 1a and 1b. The initial concentrations of both hydrogen peroxide and hexanol in the reaction phase (aqueous phase) were obtained by applying the UNIFAC (Fredenslund et al., 1975) method to estimate the thermodynamic liquid–liquid phase-equilibrium concentrations in the ternary 2-(3-) hexanol–methanol–water systems. The UNIFAC calculation method does not show any significant differences in aqueous-phase concentration of the 2-hexanol and 3-hexanol. The results calculated in conditions similar to the ones of the kinetic experiments [55°C, 4.76×10^{-2} mol of 3-hexanol and 2.50 g (30%) of H_2O_2] for the H_2O_2 and 3-hexanol concentrations in the aqueous phase are presented in Table 3a. This table shows clearly that at a constant temperature, increasing the solvent content simultaneously yields an increase in hexanol solubility and a decrease in hydrogen peroxide concentration in the aqueous phase.

An efficient way to estimate the initial rate of the hexanol oxidation reaction is first to fit the time evolution of the hexanol conversion using an empirical equation

$$X_1 = \alpha\cdot[1-\exp(-\beta\cdot t')]. \qquad (10)$$

Table 2. Catalytic Oxidation of 3-Hexanol over TS-1 Catalysts

(a) Solvent Effect*

Exp. No.	Mass of Methanol Added (g)	React. Time (h)	3-Hexanol Conv. (mol %)	H_2O_2 Conv. (mol %)	H_2O_2 Select. as Defined in Eq. 8 (mol %)
1	0.75	1	4.21	16.4	55.0
		2	5.69	23.7	53.4
		3	6.84	28.9	52.4
		4	7.86	33.9	51.3
		5	7.95	35.7	49.3
2	1.3	1	3.3	12.7	52.0
		2	4.35	20.9	46.2
		3	6.1	30.2	44.8
		4	6.96	37.8	40.7
		5	7.34	42.3	38.4
3	2.02	1	3.09	13.7	49.8
		2	4.12	20.0	45.7
		3	5.64	27.7	45.1
		4	6.30	32.4	43.1
		5	6.85	36.5	41.3
4	7.75	1	1.78	8.28	47.5
		2	2.01	12.1	36.9
		3	3.31	17.8	41.1
		4	3.34	21.9	33.8
		5	3.66	25.1	32.3

(b) Effect of Titanium Content**

Setup No.	Titanium Content Ti/(Ti+Si) (%)	React. Time (h)	3-Hexanol Conv. (mol %)	H_2O_2 Conv. (mol %)	H_2O_2 Select. as Defined in Eq. 8 (mol %)
1	1.0	1	1.32	14.1	10.6
		2	3.19	27.4	12.9
		3	4.35	36.2	13.3
		4	5.46	44.3	13.6
		5	6.51	52.0	13.8
2	1.5	1	1.71	15.4	11.1
		2	4.09	29.4	13.9
		3	5.61	42.8	13.1
		4	7.51	55.6	13.5
		5	8.29	64.3	12.9
3	1.9	1	3.28	11.3	29.1
		2	8.51	23.9	35.6
		3	11.4	32.5	35.2
		4	15.4	41.0	37.6
		5	18.2	46.4	39.4
4	2.4	1	2.86	6.80	46.7
		2	4.34	13.1	36.6
		3	5.02	15.5	35.8
		4	5.93	18.9	34.8
		5	6.38	22.4	31.5
5	4.6	1	2.50	6.60	42.1
		2	3.35	10.2	36.2
		3	4.46	13.6	36.3
		4	5.20	17.2	33.6
		5	5.52	20.1	30.5
6	6.0	1	1.46	6.33	25.6
		2	2.44	9.94	27.2
		3	3.58	14.1	28.1
		4	4.43	19.0	25.8
		5	5.05	22.8	24.5

*Reaction conditions: catalyst 125 mg; temperature #1–4: 55°C; Ti/(Ti+Si): 2.4%; 3-hexanol: 4.76×10^{-2} mol; H_2O_2: 2.20×10^{-2} mol.
**Reaction conditions: catalyst 250 mg; temperature #1–6: 55°C; no solvent used; 3-hexanol: 4.76×10^{-2} mol; H_2O_2: 4.44×10^{-2} mol.

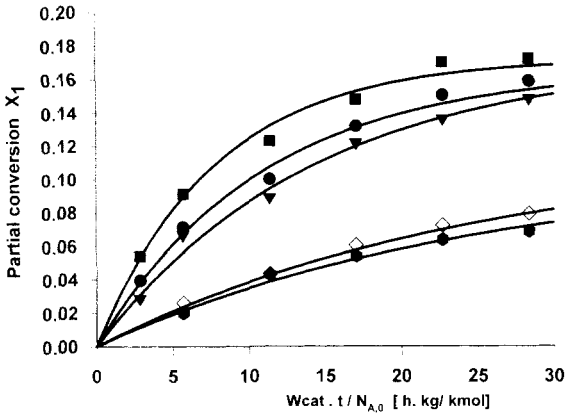

Figure 1a. Partial conversion X_1 of H_2O_2 through 3-hexanol oxidation reaction: solvent effect.

Catalyst TS-1 (2.4%); $T = 55$°C; lines: calculated according to Eq. 10; symbols: experimental values ◇ (0 g); ■ (0.75 g); ● (1.30 g); ▼ (2.0 g); ⬢ (7.75 g).

The values of the empirical parameters α and β are obtained by the Marquardt technique for the minimization of the following objective function:

$$\Phi = \sum_{i=1}^{N} w_i (X_{1C} - X_{1E})^2,$$

where w_i is a weighting factor. Figure 1a illustrates the experimental points and the lines calculated using Eq. 10 for the 3-hexanol oxidation system. It shows also the effect of added methanol solvent on the 3-hexanol oxidation rate. The calculated initial oxidation rate of 3-hexanol is therefore obtained by the derivative of Eq. 10 at $t' = 0$, that is: $(dX_1/dt')|_{t'=0} = R_0 = \alpha \cdot \beta$ (kmol/h·kg). The results for α, β, and R_0 are also reported in Table 3a. As shown from this table, the initial oxidation rate exhibits an optimal value with respect to the amount of methanol added, at 0.75 g methanol. It is interesting to note that similar observations were also reported in our previous work (Gallot et al., 1996) regarding the effect

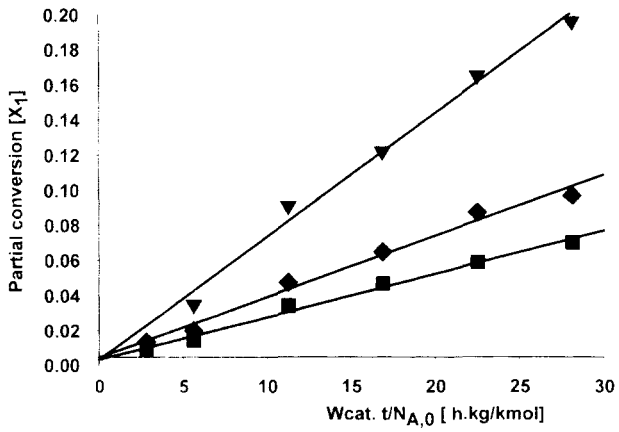

Figure 1b. Titanium content effect on partial conversion X_1.

$T = 55$°C; catalyst TS-1; symbols: ■ (1.0%); ◆ (1.5%); ▼ (1.9%).

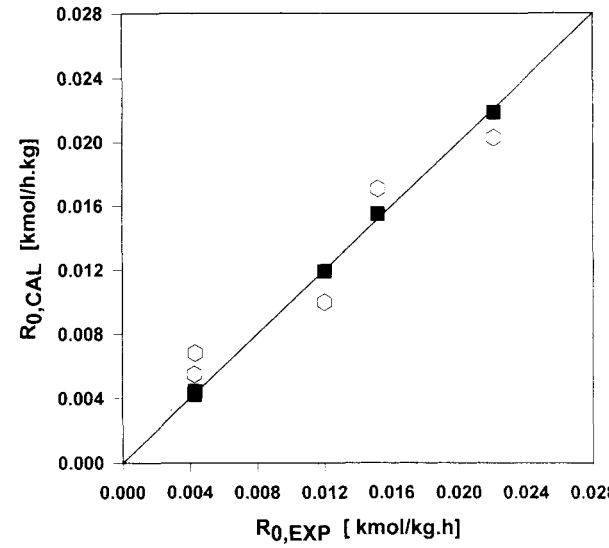

Figure 1c. Predicted vs. experimental initial oxidation rate of 3-hexanol on TS-1 (2.4%).

$T = 55$°C; ○ kinetic model (i); ■ kinetic model (iii).

of solvent addition on the initial rate of the *n*-hexane oxyfunctionalization reaction. The 3-hexanol initial oxidation rate may be expressed by the power law kinetic model:

$$R_0 = k(C_{A0})^n (C_B^{*,aq})^m. \tag{11}$$

The unknown kinetic parameters were estimated by the Marquardt minimization method of the residual sum of squares between the experimental initial rate $R_{0,E}$ and predicted $R_{0,C}$ values calculated according to Eq. 11. Thus, the partial reaction orders n and m were estimated to be 2.29 and 0.841, respectively. Again, a similar kinetic behavior has been observed in the *n*-hexane oxyfunctionalization rate, which exhibits a second reaction order with respect to H_2O_2 (Gallot et al., 1996). Moreover, the noninteger values obtained for these partial reaction orders n and m in Eq. 11 suggest the use of a Langmuir–Hinshelwood model for the kinetics of hexanol oxidation reaction. A systematic approach using different kinetic models was therefore used to explore the oxidation behavior of hexanol on titanium silicalites. The proposed kinetic models for the oxidation rate of 3-hexanol are expressed by the following equations:

$$(i)\ \text{Model 1:}\quad r = \frac{kC_A C_B^{*,aq}}{1 + K_B C_B^{*,aq}} \tag{12}$$

$$(ii)\ \text{Model 2:}\quad r = \frac{kC_A^2 C_B^{*,aq}}{1 + K_A C_A^2} \tag{13}$$

$$(iii)\ \text{Model 3:}\quad r = \frac{kC_A^2 C_B^{*,aq}}{1 + K_B C_B^{*,aq}}. \tag{14}$$

The results of the estimated kinetic parameters of each model are reported in Table 3b. The discrimination of the best kinetic model from the initial rate data was performed on the basis of a physical sense of the estimated parameters

Table 3

(a) Initial Concentrations of H_2O_2 and 3-Hexanol and Initial Rate of 3-Hexanol Oxidation, $T = 55°C$

Methanol Added (g)	C_{A0} (kmol/m^3)	$C_B^{*,aq}$ (kmol/m^3)	α	β	R_0 (kmol/h·kg)
0	9.77	0.024	4.93×10^{-2}	0.0864	4.26×10^{-3}
0.75	8.60	0.17	7.95×10^{-2}	0.278	2.21×10^{-2}
1.3	5.60	0.30	7.66×10^{-2}	0.199	1.52×10^{-2}
2.02	2.10	4.10	7.96×10^{-2}	0.151	1.20×10^{-2}
7.75	1.18	2.0	4.97×10^{-2}	0.0865	4.30×10^{-3}

(b) Estimated Kinetic Parameters for the Proposed Kinetic Models for the Initial Rates of 3-Hexanol, $T = 55°C$

Kinetic Models	Kinetic Const.	Est. Value	95% Confidence Intervals		T-Value	F-Ratio*
			Lower Limit	Upper Limit		
(i)	k (m^6/kg·h·kmol)	2.271×10^{-2}	0.2028×10^{-2}	0.4340×10^{-1}	3.60	70.18
	K_B (m^3/kmol)	5.668	−1.755	13.13	2.21	
(ii)	k (m^9/kg·h·kmol^2)	8.250×10^{-3}	3.603×10^{-4}	1.289×10^{-3}	—	—
	K_A m^3/kmol	-6.216×10^{-3}	-1.054×10^{-2}	-1.888×10^{-3}		
(iii)	k (m^9/kg·h·kmol^2)	1.866×10^{-3}	1.783×10^{-3}	1.950×10^{-3}	91.7	7,361.9
	K_B (m^3/kmol)	0.455	0.399	0.5107	25.6	

Note: $A = H_2O_2$; B = 3-hexanol.
*F − ratio = $\{(\Sigma_i R_{c,i}^2/p)/[\Sigma_i(R_{c,i} - R_{E,i})^2/N - p]\}$.

and the F-statistics. Thus, kinetic model (ii) can be discarded because of the negative value calculated for the adsorption constant K_A. Table 3b also indicates that at the probability level of 95% and the given degrees of freedom, the remaining two kinetic models [model (i) and model (iii)] satisfy the necessary condition: $F > Fc = 9.55$ (not to be rejected). Kinetic model (i) may also be excluded because the lower limit of the adsorption constant K_B has a negative value. Moreover, Figure 1c compares the predicted and experimental initial rate of 3-hexanol oxidation according to kinetic models (i) and (iii). From this figure, it is obvious that model (iii) yields the best representation of initial rate data. Thus, the catalytic oxidation-rate behavior of 3-hexanol can be described by the empirical-rate equation (Eq. 14).

Kinetic modeling of hexanol oxidation reaction

In an attempt to get more precise and quantitative information on the catalytic oxidation reaction of 2-(3-) hexanol on TS, the time evolution of the reaction system will now be analyzed. Thus, the mass balance of 2-(3-) hexanone and oxygen production are expressed in terms of the following two ordinary differential equations:

$$\frac{dX_{1,i}}{dt} = \frac{W\text{cat}}{N_{A0}} \cdot R_{1,i} \tag{15}$$

$$\frac{dX_{2,i}}{dt} = 2 \cdot \frac{W\text{cat}}{N_{A0}} \cdot R_{2,i} \tag{16}$$

where

$$R_{1,i} = \frac{k_{1,i} \cdot K_{Bi} \cdot C_i^{*,aq} \cdot C_A^2}{1 + K_{Bi} \cdot C_i^{*,aq}} \tag{17}$$

is the rate of Reaction 2 deduced from the empirical equation (Eq. 14), $k_{1,i}$ the kinetic constant, and K_{Bi} the adsorption constant of component i (i stands for 2-hexanol or 3-hexanol). Equation 17 is identical to the rate equation found for hexanols oxidation in the analysis of n-hexane oxidation by H_2O_2 on the same catalysts (Gallot et al., 1996, 1997).

As to the rates of O_2 formation $R_{2,i}$, two different contributions will be considered depending on whether or not extraframework Ti is present in the catalyst. As discussed in Gallot et al. (1997), when all Ti is in substitutional framework position (Ti/(Ti+Si) ≤ 1.9%), oxygen is only generated during the activation step for the reaction between hexanol and hydrogen peroxide. As shown below, when this step is rate limiting, the rate of oxygen generation can be expressed as

$$R_{2,i}^* = \frac{k_{2,i} C_A^2}{1 + K_{Bi} C_i^{*,aq}}. \tag{18a}$$

In cases where extraframework Ti is also present (Ti/(Ti+Si) > 1.9%), hydrogen peroxide is also decomposed on extraframework sites by a 0.5-order reaction (Gallot et al., 1997):

$$R_{2,i} = R_{2,i}^* + k_d C_A^{0.5}, \tag{18b}$$

where k_d is the H_2O_2 decomposition rate constant on extraframework Ti, which is written in the following expression: $k_d = k_{d,0} \exp(-E_d/RT)$. Using TS-1 with 2.4% Ti/(Ti+Si) as a catalyst, the preexponential factor $k_{d,0}$ and the activa-

Table 4. Results for the Estimated Kinetic Parameters

(a) Reaction Conditions Used

Reaction System	Temp. (°C)	Methanol Added (g)	Init. Mol of Alcohol (mol)	Mol of H_2O_2 (mol)	Catal. Wt. (g) (TS-1 2.4%)
2-Hexanol	45, 55, 60, and 65	2.1	4.76×10^{-2}	2.20×10^{-2}	0.125
3-Hexanol	45, 55, 60, and 70	2.1	4.76×10^{-2}	2.20×10^{-2}	0.125

(b) Reduced Kinetic Parameters

Parameter	Est.	Std. Error	Asymptotic Covariance Matrix					
			$\varphi_{1,3}$	$\varphi_{2,3}$	$\varphi_{3,3}$	$\psi_{1,3}$	ψ_2	$\psi_{3,3}$
$\varphi_{1,3}$	−8.06	0.14	1.00					
$\varphi_{2,3}$	−5.84	0.16	0.325	1.00				
$\varphi_{3,3}$	0.434	0.06	−0.087	−0.322	1.00			
$\psi_{1,3}$	8.92	0.02	0.944	0.045	−0.411	1.00		
ψ_2	7.45	0.28	−0.045	0.096	0.257	0.287	1.00	
$\psi_{3,3}$	-2.34×10^{3}	0.55×10^{3}	0.68×10^{-4}	0.68×10^{-4}	-2.33×10^{-6}	-0.37×10^{-6}	-3.6×10^{-4}	1.00

(c) Physical Parameters

Compound (i)	$k_{1,i,0}^{app}$ ($m^9\cdot kmol^{-2}\cdot kg^{-1}\cdot h^{-1}$)	$E_{1,i}^{app}$ (kcal/mol)	$\Delta S_{a,i}$ (cal/mol·K)	$\Delta H_{a,i}$ (kcal/mol)	$E_{1,i}$ (kcal/mol)
2-Hexanol	4.37×10^{6}	10.3	−29.0	−9.2	**19.5**
3-Hexanol	1.20×10^{7}	14.8	−13.3	−4.6	**19.4**

tion energy E_i/R were found to be, respectively, 7.87×10^{7} $m^{1.5}\cdot kmol^{0.5}\cdot kg^{-1}\cdot h^{-1}$ and 8.18×10^{3} (Gallot et al., 1997).

The reactor model, the system of two ordinary differential equations (ODE) described in Eqs. 15–16, was solved numerically using the backward-difference method (IMSL, 1995) with the initial reaction condition $[X_1, X_2]^T = [0,0]^T$. The numerical estimation of the kinetic constants was performed with an adaptive nonlinear least-squares algorithm, the Gauss–Newton–Marquardt technique (Seinfeld and Lapidus, 1978; IMSL, 1995), which minimized the residual sum of squares (RSS) between the experimental and estimated partial conversions of H_2O_2.

The time-dependent kinetic results from the 2-hexanol and 3-hexanol oxidation reactions at the conditions summarized in Table 4a were used to estimate the following kinetic parameters in rate Eqs. 17 and 18:

$$k_{1,i}^{app} = k_{1,i,0}^{app}\exp(-E_{1,i}^{app}/RT) \tag{19a}$$

$$k_{2,i} = k_{2,i,0}\exp(-E_{2,i}/RT) \tag{19b}$$

$$K_{Bi} = \exp(\Delta S_{a,i}/R)\exp(-\Delta H_{a,i}/RT), \tag{19c}$$

where $k_{1,i}^{app} = k_{1,i}K_{Bi}$; $k_{1,i,0}^{app}$, $k_{2,i,0}$ are the preexponential factors; $E_{1,i}^{app}$, $E_{2,i}$ the activation energies; $\Delta S_{a,i}$ the adsorption entropies; and $\Delta H_{a,i}$ the adsorption enthalpies, $i = 2$ for 2-hexanol and $i = 3$ for 3-hexanol.

In order to reduce the high correlation between the preexponential factors and the activation energies or between the entropies and the heats of adsorption, the following reparameterization (Pritchard and Bacon, 1978) was adopted in the present work:

$$\varphi_{n,i} = \ln(k_{n,i,0}) - E_{n,i}/RT_{ref} \tag{20a}$$

$$\psi_{n,i} = \ln(E_{n,i}/R) \quad (n = 1,2) \tag{20b}$$

and

$$\varphi_{3,i} = \frac{\Delta S_{a,i}}{R} - \frac{\Delta H_{a,i}}{RT_{ref}}, \quad \psi_{3,i} = -\frac{\Delta H_{a,i}}{R}, \quad i = 2\text{-,3-hexanol}, \tag{20c}$$

where T_{ref} is the reference temperature set to 298 K.

The statistical estimates of these parameters are shown in Tables 4b and 4c for the 3-hexanol oxidation system. The method of bisection was used to illustrate the goodness of fit for H_2O_2 partial conversions, X_1 and X_2. Thus, the predicted values of X_1 and X_2 were compared with the experimental ones. The results are illustrated in Figures 2a and 2b for the 2-hexanol oxidation and in Figures 3a and 3b for the 3-hexanol oxidation reaction, respectively. It follows from these figures that the rate expressions given earlier are consistent with the experimental observations under the reaction conditions investigated. The oxidation rates of 2- (3-) hexanol on TS-1 have a Langmuir-type dependence on the alcohol concentration in the aqueous phase, described by Eq. 17. This type of rate behavior is common in heterogeneous catalysis systems and typically indicates that the rate-controlling step of the oxidation reaction may involve a species that is in adsorption equilibrium on an active site of the TS directly in contact with the aqueous phase.

The temperature dependence of the apparent kinetic constants, $k_{1,i}^{app} = k_{1,i}\cdot K_{Bi}$, $i = 2$- and 3-hexanol and adsorption equilibrium constants K_{Bi} are illustrated in Figures 4a and 4b and in Figures 5a and 5b, respectively, for 2-hexanol and 3-hexanol reaction systems. Within the scatter of the data, the apparent kinetic constants $k_{1,i}^{app}$ follow the Arrhenius form, and have activation energy values of 10.3 and 14.8 kcal/mol for 2-hexanol and 3-hexanol oxidation reactions, respectively. An interesting result is the similarity of the activation energy observed in the elementary reaction constants $k_{1,i}$

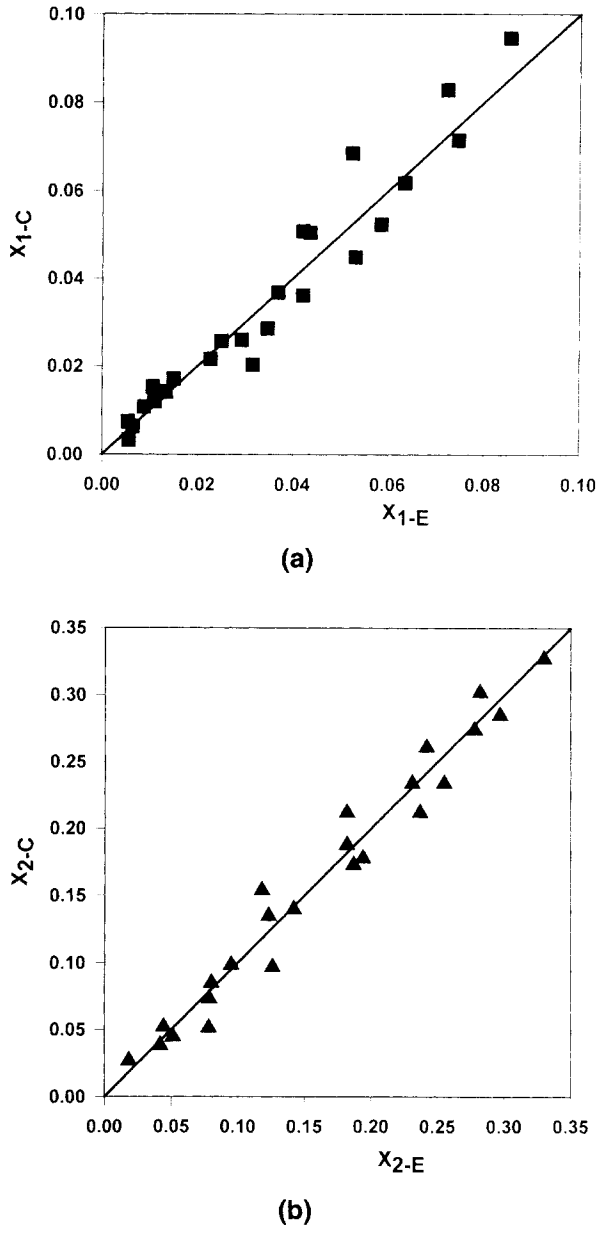

Figure 2. Predicted vs. experimental partial conversions of H_2O_2 in 2-hexanol oxidation reaction.

(a) Partial conversion X_1; (b) partial conversion X_2.

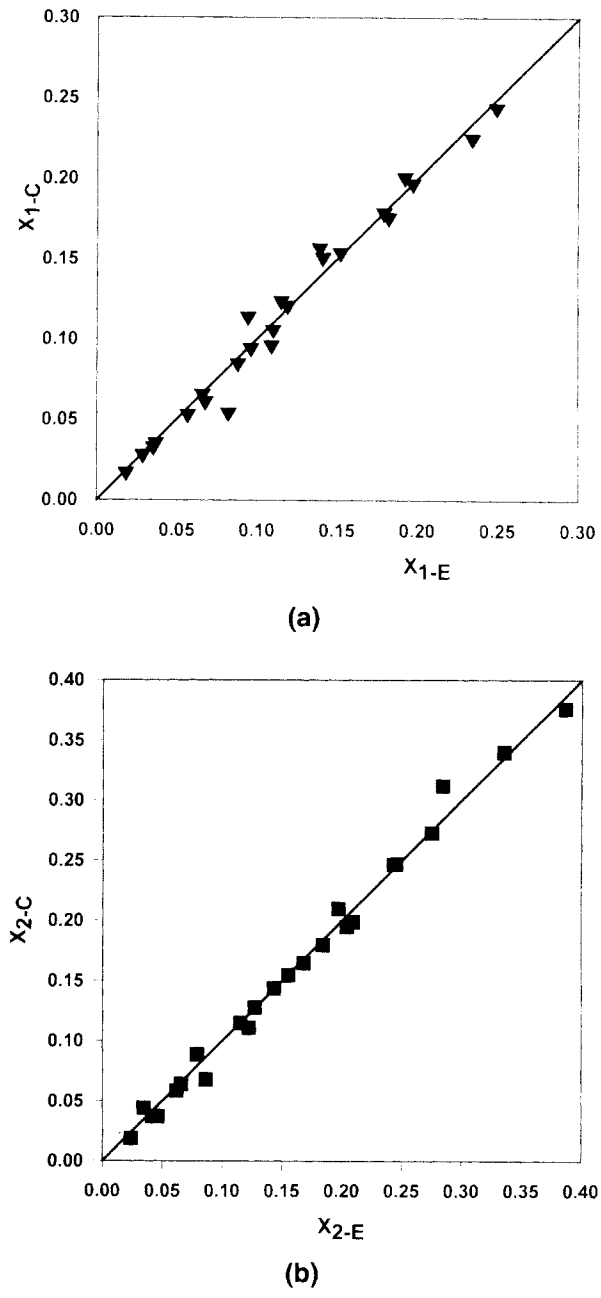

Figure 3. Predicted vs. experimental partial conversions of H_2O_2 in 3-hexanol oxidation reaction.

(a) Partial conversion X_1; (b) partial conversion X_2.

$[E_{1,i} = E_{1,i}^{app} + (-\Delta H_i)]$ for both oxidation of 2- and 3-hexanols 19.5 and 19.4 kcal/mol, respectively. It may be concluded that both oxidation reactions can have the same rate controlling step.

The 2-hexanol and 3-hexanol adsorption constants vs. reaction temperature are shown in Figures 4a and 5a, respectively. The estimated adsorption constant values are reported in Table 4c. These values are indicative of a relatively weak bond but immobile chemisorbed state of 2-hexanol and 3-hexanol on the surface active site of TS-1 catalyst. It can be seen from this table, however, that 2-hexanol has a higher constant adsorption value than 3-hexanol. This shows that the adsorption of 2-hexanol on a TS active site may involve some relatively more stable species than adsorbed 3-hexanol.

The proposed kinetic model of 2- (3-) hexanol oxidation reaction as described in Eq. 17 was used to predict experimental results under the following reaction conditions: methanol solvent added: 0–7.75 g; temperature 55°C; H_2O_2: hexanol mole ratio: 1:2.16; H_2O_2: 0.0221 mol. Good agreement between simulated partial conversions of H_2O_2 and experimental ones can be observed from Figures 6a and 6b and Figures 7a and 7b. It confirms the second reaction order with respect to H_2O_2 concentration, as described by Eq. 17. It is interesting to notice that such oxidation reaction behavior was also observed in the previously reported case of *n*-hexane oxyfunctionalization reaction on the TS samples (Gallot et

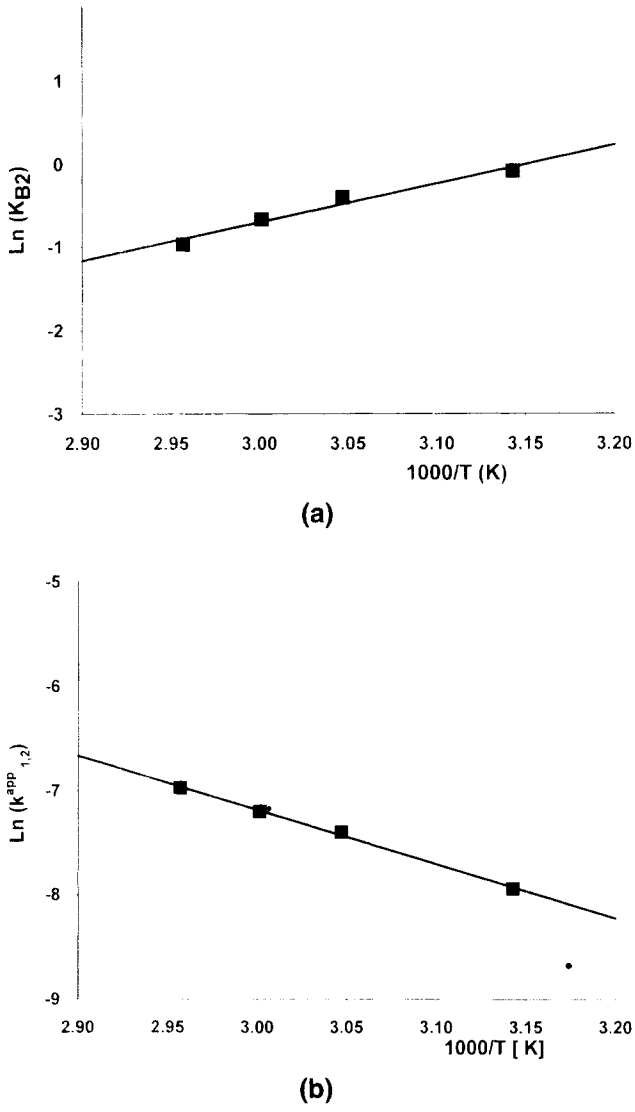

Figure 4. Temperature dependence of estimated kinetic parameters in 2-hexanol oxidation rate.

(a) Adsorption constant K_{B2} of 2-hexanol; (b) apparent kinetic constant k_{12}^{app}.

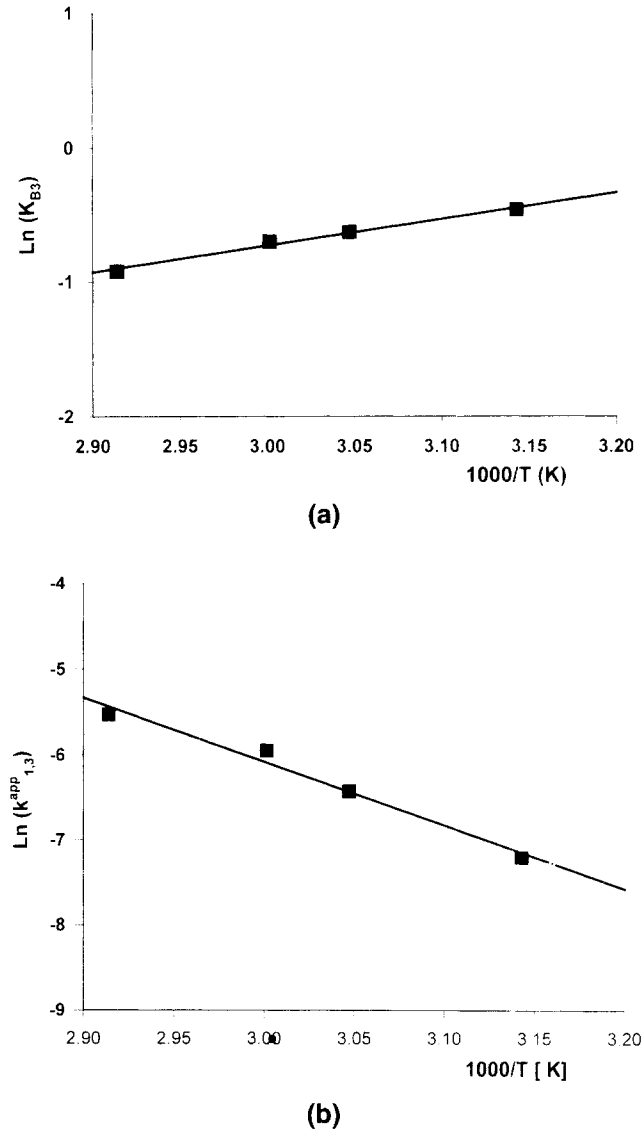

Figure 5. Temperature dependence of estimated kinetic parameters in 3-hexanol oxidation rate.

(a) Adsorption constant K_{B3} of 3-hexanol; (b) apparent kinetic constant k_{13}^{app}.

al., 1996, 1997; Fu and Kaliaguine, 1994). Such behavior may be explained by the observation that the same catalytic site and same rate-controlling steps are involved in the activation of *n*-hexane and the hexanols on titanium silicalites.

The effect of Ti contents on the oxidation reaction rate of 3-hexanol at 55°C was also investigated. Results are reported in Figure 8. As can be seen from this figure, the activity of TS-1 toward 3-hexanol oxidation increases with Ti content up to 1.9% Ti/(Ti+Si). A further increase in Ti content, which according to UV-visible spectra of the catalysts (Gallot et al., 1997) corresponds to the appearance of extraframework Ti species, does not result in an increased rate constant. Such an observation was also reported in our previous work (Gallot et al., 1997) for the rate of the *n*-hexane reaction. It was indeed concluded that a partial coverage of the active framework Ti site by inactive extraframework Ti species was the main reason for the drop in the catalyst activity toward the oxidation reaction.

Mechanistic implications in hexanol oxidation

The kinetic results observed in the work for the partial oxidation of hexanols are strikingly similar to the ones established in our previous works for *n*-hexane oxyfunctionalization over titanium silicalites. In these previous investigations Eq. 17 is essentially identical to the expressions derived for *n*-hexane primary oxidation and hexanols secondary rates (Eqs. 15 and 16) in Gallot et al. (1997). Moreover, the proportionality of the kinetic constants to Ti content (Figure 8), up to a value of Ti/(Ti+Si) = 1.9%, was also observed in this previous work.

In spite of these similarities, what follows results from a new investigation of possible mechanism that should lead not only to Eq. 17 but to a correct description of the experimental H_2O_2 selectivities reported in Tables 1 and 2.

A possible reaction mechanism, summarized in Scheme 1, likely proceeds by a heterolytic abstraction of α-H by a tita-

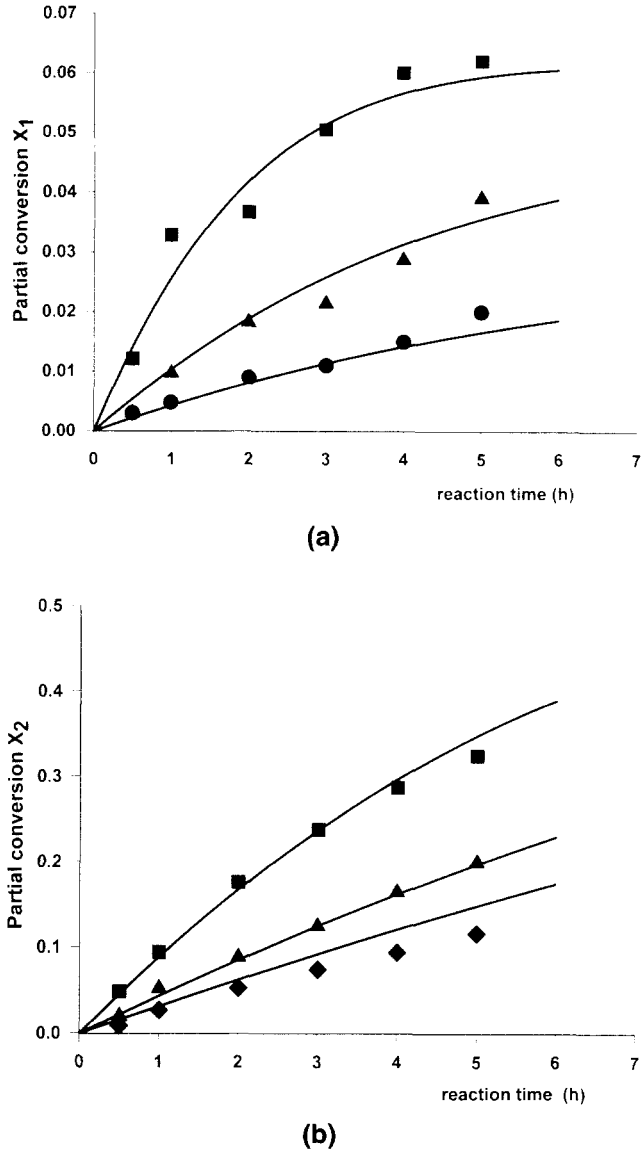

Figure 6. Simulation of H_2O_2 partial conversions in 2-hexanol oxidation reaction.

Catalyst TS-1 (2.4%); $T = 55$°C. (a) Partial conversion X_1; (b) partial conversion X_2. Lines: predicted values. Symbols: experimental with methanol solvent: ■ (1.25 g); ▲ (2.02 g); ● (4.0 g).

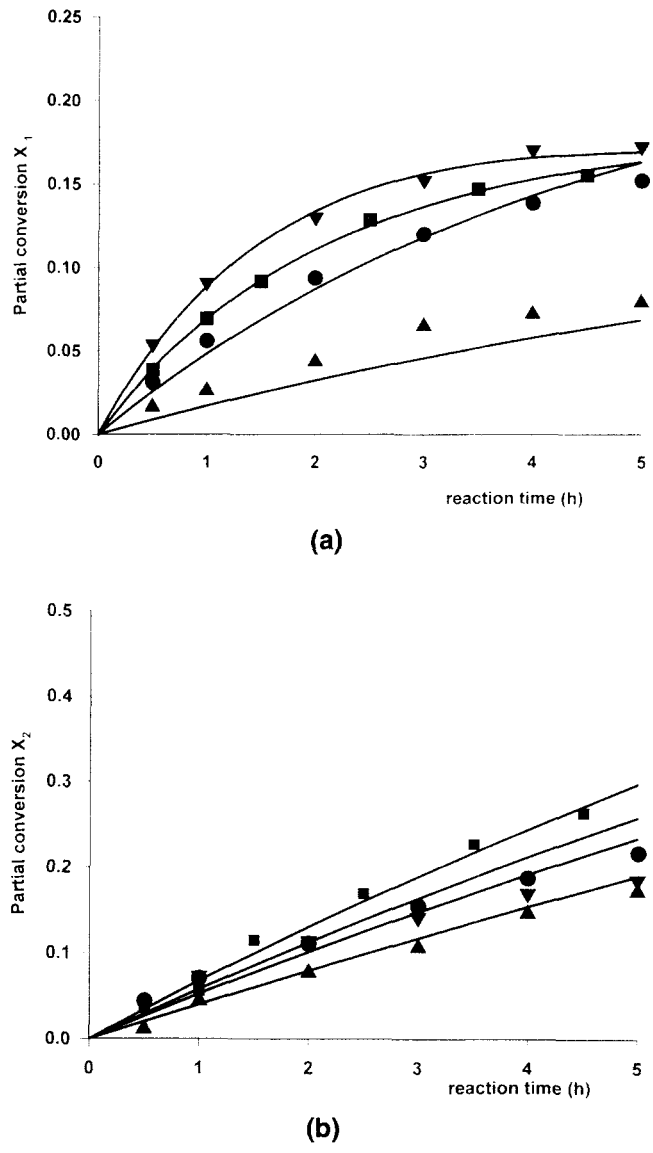

Figure 7. Simulation of H_2O_2 partial conversions in 3-hexanol oxidation reaction.

Catalyst TS-1 (2.4%); $T = 55$°C. (a) Partial conversion X_1; (b) partial conversion X_2. Lines: predicted values. Symbols: experimental with methanol solvent: ▼ (0.75 g); ■ (1.30 g); ● (2.02 g); ▲ (7.75 g).

nium peroxo group. Step (i) is the activation of titanium in the framework position [site (T1)] by one molecule H_2O_2 to form a titanium hydroperoxo complex [site (S2)]. Several experimental facts supported by spectroscopic studies have indeed demonstrated the interaction of aqueous H_2O_2 on TS catalysts. UV-visible spectra, for example, have indicated an apparition in the presence of H_2O_2, a band at 26,000 cm^{-1} that was ascribed to the characteristic absorption of the hydroperoxo group (Geobaldo et al., 1992; Zecchina et al., 1991). It was also reported by Huybrechts et al. (1991) that the characteristic IR band at 960 cm^{-1} disappears when TS is exposed to aqueous H_2O_2, and this band reappears when this catalyst is heated at 330 K.

Hexanol diffuses within the zeolite pores and is then adsorbed on this complex site, according to step (ii). Thus, two hydrogen atoms are abstracted by the titanium hydroperoxo group: one atom is the α-H and the other one is from the functional group OH of hexanol to produce one mole of water and an adsorbed form of the corresponding hexanone [step (iii)]. The ketone desorption generates a titanium hydroxy group [site (S5)] that may react with H_2O_2 to restore the titanium hydroperoxo complex [site (S2)]. Two other cycles may also be closed following the surface rearrangement of the silanol defects group with either the titanium hydroperoxo site [step (vi)] or the titanium hydroxy group [step (vii)]. Step (vi) results in the formation of oxygen gas, which is consistent with our experimental observations.

According to this mechanism, the oxidation reaction of 2- and 3-hexanols on framework titanium may therefore be illustrated by the following linear graph:

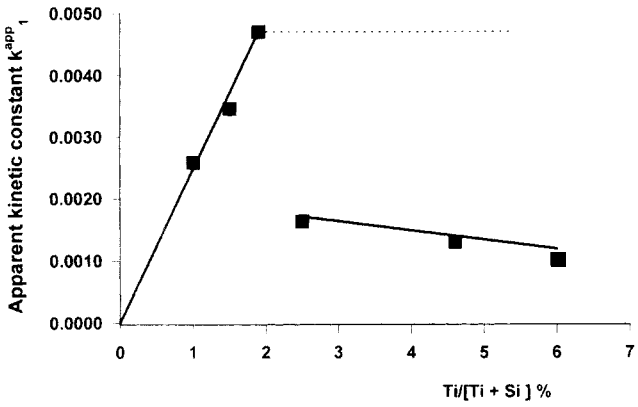

Figure 8. Correlation between 3-hexanol oxidation kinetic rate constant $k_{1,3}$ and the Ti content of TS-1 catalyst, $T = 55°C$.

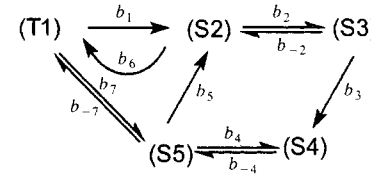

where b_1, b_2, b_{-2}, b_3, b_4, b_{-4}, b_5, b_6, b_7, and b_{-7} are the weights of the graph defined as

$$b_1 = k_{c1}C_A, \quad b_2 = k_{c2}C_i^{*,aq}, \quad b_3 = k_{c3}, \quad b_{-2} = k_{c-2},$$
$$b_4 = k_{c4}, \quad b_{-4} = k_{c-4}C_D = 0, \quad b_5 = k_{c5}C_A, \quad b_6 = k_{c6},$$
$$b_7 = k_{c7}, \quad b_{-7} = k_{c-7}.$$

With the assumption that the surface intermediates (T1), (S2), (S3), (S4), and (S5) are in steady-state concentrations and that

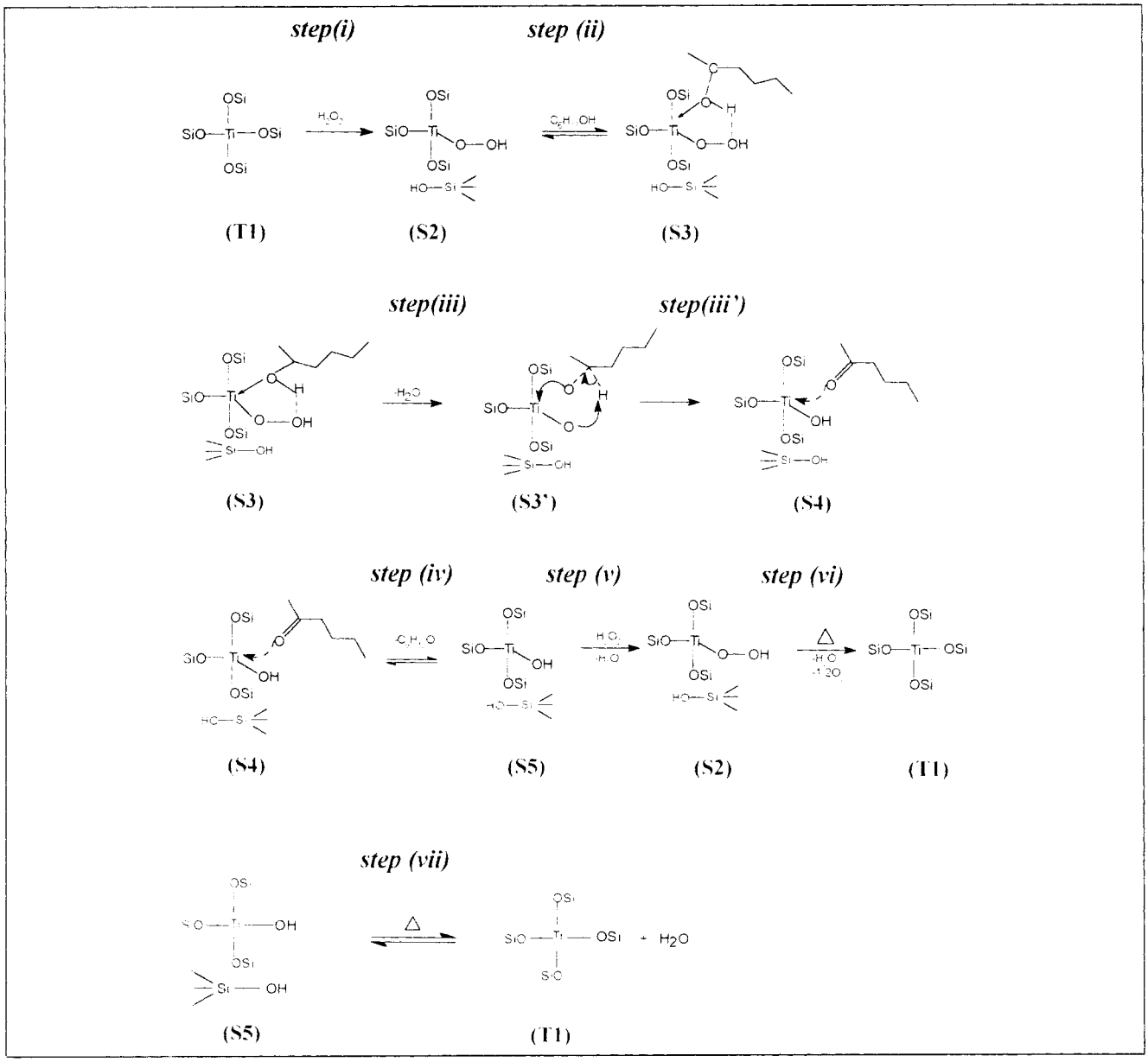

Scheme 1.

$b_1, b_5 \ll b_k$, $k = -2, -7, 2-7$, the rates of Reactions 2 and 3 will be expressed as

$$R_{1,i} = \frac{b_2 b_3 b_4 (b_1 b_5 + b_5 b_{-7})}{(b_{-2} b_4 b_6 b_7 + b_2 b_3 b_4 b_{-7} + b_2 b_3 b_{-4} b_{-7})} \quad (21)$$

$$R_{2,i} = \frac{b_1 b_5 b_6 (b_3 b_4 + b_{-2} b_4) + b_{-2} b_4 b_5 b_6 b_{-7}}{(b_{-2} b_4 b_6 b_7 + b_2 b_3 b_4 b_{-7} + b_2 b_3 b_{-4} b_{-7})}. \quad (22)$$

Replacing the b_i weight values in the preceding equations, the rate expressions will be:

$$R_{1,i} = \frac{\dfrac{k_{c2} k_{c3}}{k_{c-2} k_{c6}} \cdot \left(\dfrac{k_{c1} k_{c5}}{k_{c7}} C_A + \dfrac{k_{c5} k_{c-7}}{k_{c7}} \right) \cdot C_A C_i^{*,\mathrm{aq}}}{1 + \dfrac{k_{c2}}{k_{c-2}} \cdot \dfrac{k_{c3}}{k_{c6}} C_i^{*,\mathrm{aq}}} \quad (23)$$

$$R_{2,i} = \frac{\dfrac{k_{c1} k_{c5} (k_{c3} + k_{c-2})}{k_{c-2} k_{c-7}} C_A^2 + \dfrac{k_{c5} k_{c-7}}{k_{c7}} C_A}{1 + \dfrac{k_{c2}}{k_{c-2}} \cdot \dfrac{k_{c3}}{k_{c6}} \cdot C_i^{*,\mathrm{aq}}}. \quad (24)$$

Let

$$k_{11} = \frac{k_{c1} k_{c5}}{k_{c7}}, \quad K_{Bi} = \frac{k_{c2}}{k_{c-2}} \cdot k_r, \quad k_{12} = \frac{k_{c5} k_{c-7}}{k_{c7}},$$

$$k_r = \frac{k_{c3}}{k_{c6}}, \quad k_{21} = \left(1 + \frac{k_{c3}}{k_{c-2}} \right) k_{11}.$$

Thus Eqs. 23 and 24 are reduced to

$$R_{1,i} = \frac{k_{11} \cdot K_{Bi} \cdot C_A \cdot C_i^{*,\mathrm{aq}} \cdot (1 + k_{12} C_A)}{(1 + K_{Bi} C_i^{*,\mathrm{aq}})} \quad (25)$$

$$R_{2,i} = \frac{k_{21} \cdot C_A \cdot (1 + k_{12} C_A)}{(1 + K_{Bi} C_i^{*,\mathrm{aq}})}. \quad (26)$$

Equations 25 and 26 describe the catalytic oxidation rates of hexanols and further decomposition of H_2O_2 on the titanium framework site.

In the proposed mechanism (Scheme 1), H_2O_2 decomposition on framework Ti is through steps (v) and (vi). Thus, the presence of the so-called open tetrahedral Ti site [$(OSi)_3TiOH$] is detrimental to H_2O_2 selectivity, as it promotes step (v). High concentrations of silanol groups in the neighborhood of framework Ti would also yield high rates of H_2O_2 decomposition through step (vi).

It is therefore concluded that even in the absence of the extraframework Ti phase, H_2O_2 selectivity would be improved by preparation techniques that minimize the content in surface-defect silanol groups. This conclusion is consistent with the experimental observations of Uguina et al. (1995). Indeed, these authors reported that the H_2O_2 selectivity in the *n*-hexane oxyfunctionalization reaction was greatly affected when TS-1 catalysts prepared from different synthesis variables, for example, the OH^-/SiO_2 ratio in the cogel, were used.

n-Hexane oxyfunctionalization

Mechanistic Implications in n-Hexane Oxyfunctionalization. The objective of the following section is to develop a kinetic model extending the one previously reported for hexanols to an *n*-hexane oxyfunctionalization scheme. At this point, however, the rate equations will be derived on the basis of a graph (Yablonskii et al., 1991) that does not differentiate between 2- and 3-hexanols or 2- and 3-hexanones. This graph is based on the mechanism shown as Scheme 2. The elementary reaction steps and the matrix of intermediate stoichiometric coefficients (MISC) are given in Table 5.

Steps (i) through (vii) are similar to those described in the preceding hexanol oxidation section (Scheme 1). Step (viii) is the reaction of *n*-hexane with the hydroperoxo complex site (S2) to form the intermediate cyclic compound (S6), which involves the agostic bond

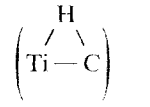

(Gallot et al., 1996). Then, the adsorbed intermediate (S6) can react in two different ways, either by desorption, forming 2- or 3-hexanol [step (ix)], or by further reacting with H_2O_2 to yield 2- or 3-hexanone by a direct parallel route with no intermediate formation of hexanol [step (xi–xii)].

As seen from the MISC (Table 5), it seems that there are eight chemical routes (designated as N_I to N_{VIII}):

$$C_6H_{14} + H_2O_2 \rightarrow C_6H_{13}OH + H_2O \quad (N_I \text{ and } N_{IV})$$

$$C_6H_{13}OH + H_2O_2 \rightarrow C_6H_{12}O + 2H_2O \quad (N_{II} \text{ and } N_V)$$

$$C_6H_{14} + 2H_2O_2 \rightarrow C_6H_{12}O + 3H_2O \quad (N_{III} \text{ and } N_{VI})$$

$$H_2O_2 \rightarrow H_2O + 1/2O_2\,(g). \quad (N_{VII} \text{ and } N_{VIII})$$

Similar reaction routes (for example, I and IV) may involve either the closed (T1) or open (S5) tetrahedral Ti sites. The experiments performed separately with 2- and 3-hexanol have shown that no isomerization reactions (2-OL $\rightleftharpoons$ 3-OL, 2-OL $\rightleftharpoons$ 3-ONE, 3-OL $\rightleftharpoons$ 2-ONE, 2 ONE $\rightleftharpoons$ 3ONE) occur during the oxidation process. Moreover, one can establish that the separate *n*-hexane oxidation routes

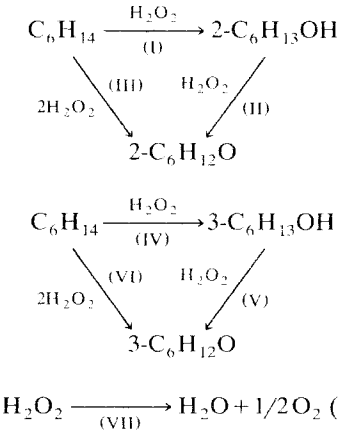

$$H_2O_2 \xrightarrow[(VII)]{} H_2O + 1/2O_2\,(g)$$

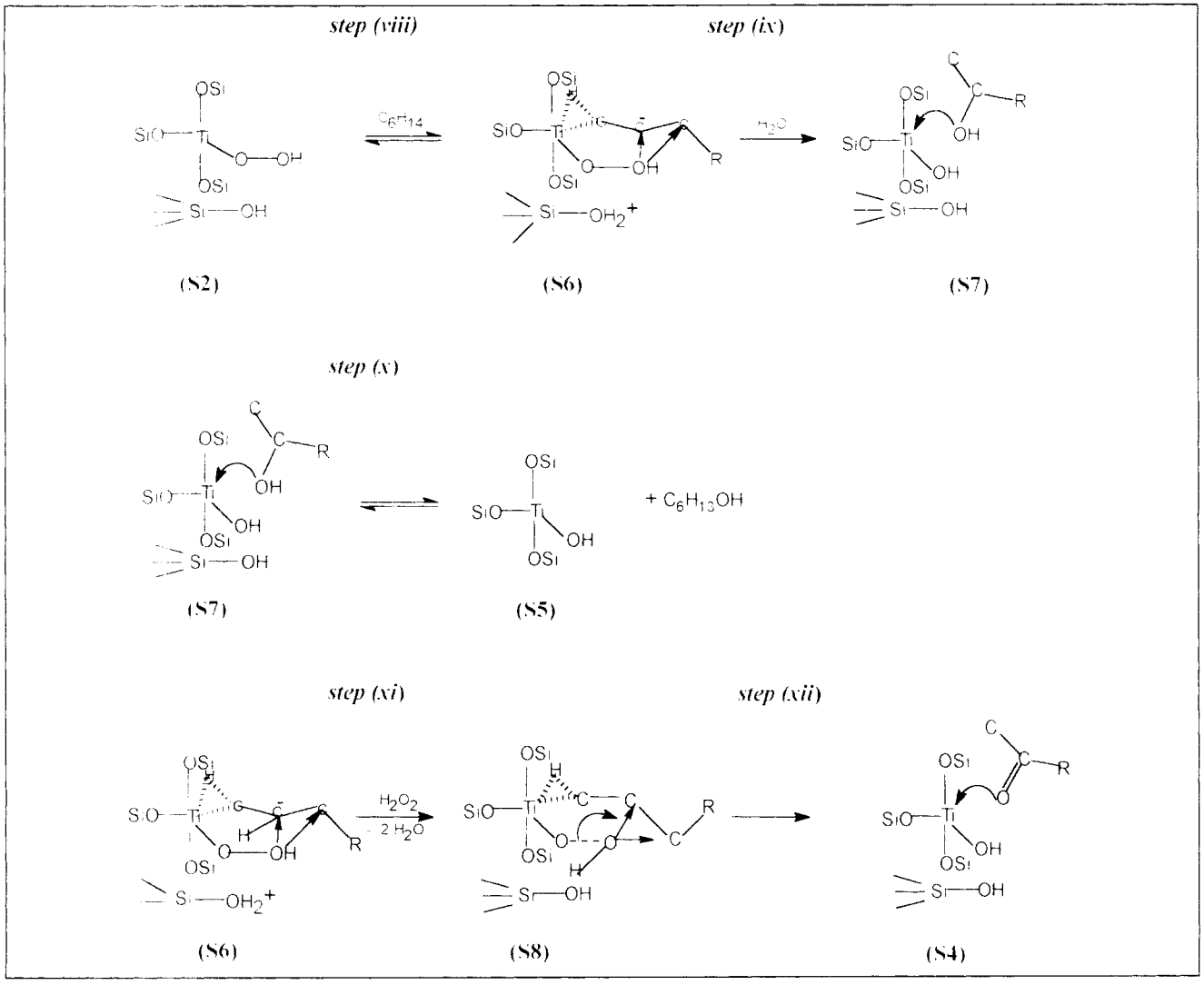

Scheme 2.

follow the rate equations derived from the preceding graph. This will be fully demonstrated in a future work.

The graph theory (Yablonskii et al., 1991) was used to find the rate expressions R_i (i = I–VII) for the preceding seven reactions. These equations were derived under the assumption that the surface intermediates (T1), (S2)–(S7) are in steady-state concentrations and the graph weights b_i satisfy the following conditions:

Table 5. Elementary Reaction Steps of *n*-Hexane Oxyfunctionalization on Framework Ti Site (Scheme 2)

Step	Elementary Reaction	Graph Wt. b_i	Routes							
			I	II	III	IV	V	VI	VII	VIII
i	$H_2O_2 + (T1) \rightarrow (S2)$	$k_{c1}C_A$	0	0	1	1	1	0	1	0
ii	$C_6H_{13}OH + (S2) \rightleftharpoons (S3)$	$k_{c2}C_B$, kc_{-2}	0	1	0	0	1	0	0	0
iii	$(S3) \rightarrow (S4) + H_2O$	k_{c3}	0	1	0	0	1	0	0	0
iv	$(S4) \rightleftharpoons (S5) + C_6H_{12}O$	k_{c4}, k_{c-4}	0	1	1	0	1	1	0	0
v	$H_2O_2 + (S5) \rightarrow (S2) + H_2O$	$k_{c5}C_A$	1	1	0	0	0	1	0	1
vi	$(S2) \rightarrow (T1) + H_2O + 1/2O_2$ (g)	k_{c6}	0	0	0	0	0	0	1	1
vii	$(T1) + H_2O \rightleftharpoons (S5)$	k_{c7}, k_{c-7}	0	0	−1	−1	−1	0	0	1
viii	$C_6H_{13} + (S2) \rightleftharpoons (S6)$	$k_{c8}C_H$, k_{c-8}	1	0	1	1	0	1	0	0
ix	$(S6) \rightarrow (S7)$	k_{c9}	1	0	0	1	0	0	0	0
x	$(S7) \rightarrow (S5) + C_6H_{13}OH$	k_{c10}	1	0	0	1	0	0	0	0
xi	$H_2O_2 + (S6) \rightarrow (S8) + 2H_2O$	$k_{c11}C_A$	0	0	1	0	0	1	0	0
xii	$(S8) \rightarrow (S4)$	k_{c12}	0	0	1	0	0	1	0	0

$$\prod_{m,n} b_m b_n b_\alpha b_2 \ll \prod_{i,j,k,l} b_i b_j b_k b_l \quad (n, \alpha = 1 \text{ and/or } 5,\ n \neq \alpha)$$

$$\prod_{m,n} b_m b_n b_\alpha b_8 \ll \prod_{i,j,k,l} b_i b_j b_k b_l \quad (n, \alpha = 1 \text{ and/or } 5,\ n \neq \alpha),$$

In other words steps (i) or (v) are rate limiting.

The rates of reaction (I) through reaction (VII) are then expressed as

$$R_{\mathrm{I}} = \frac{k_{11} K_H C_H^{*,\mathrm{aq}} C_A (k_{12} C_A + k_{13})}{(1 + K_H \cdot C_H^{*,\mathrm{aq}} + K_{B2} \cdot C_{B2}^{*,\mathrm{aq}} + K_{B3} \cdot C_{B3}^{*,\mathrm{aq}} + K_P C_A^2)} \tag{27}$$

$$R_{\mathrm{II}} = \frac{k_{21} K_{B2} C_{B2}^{*,\mathrm{aq}} C_A (k_{22} C_A + k_{23})}{(1 + K_H \cdot C_H^{*,\mathrm{aq}} + K_{B2} \cdot C_{B2}^{*,\mathrm{aq}} + K_{B3} \cdot C_{B3}^{*,\mathrm{aq}} + K_P C_A^2)} \tag{28}$$

$$R_{\mathrm{III}} = \frac{k_{31} K_H C_H^{*,\mathrm{aq}} C_A (k_{32} C_A + k_{33})}{(1 + K_H \cdot C_H^{*,\mathrm{aq}} + K_{B2} \cdot C_{B2}^{*,\mathrm{aq}} + K_{B3} \cdot C_{B3}^{*,\mathrm{aq}} + K_P C_A^2)} \tag{29}$$

$$R_{\mathrm{IV}} = \frac{k_{41} K_H C_H^{*,\mathrm{aq}} C_A (k_{42} C_A + k_{43})}{(1 + K_H \cdot C_H^{*,\mathrm{aq}} + K_{B2} \cdot C_{B2}^{*,\mathrm{aq}} + K_{B3} \cdot C_{B3}^{*,\mathrm{aq}} + K_P C_A^2)} \tag{30}$$

$$R_{\mathrm{V}} = \frac{k_{51} K_{B3} C_{B3}^{*,\mathrm{aq}} C_A (k_{52} C_A + k_{53})}{(1 + K_H \cdot C_H^{*,\mathrm{aq}} + K_{B2} \cdot C_{B2}^{*,\mathrm{aq}} + K_{B3} \cdot C_{B3}^{*,\mathrm{aq}} + K_P C_A^2)} \tag{31}$$

$$R_{\mathrm{VI}} = \frac{k_{61} K_H C_H^{*,\mathrm{aq}} C_A (k_{62} C_A + k_{63})}{(1 + K_H \cdot C_H^{*,\mathrm{aq}} + K_{B2} \cdot C_{B2}^{*,\mathrm{aq}} + K_{B3} \cdot C_{B3}^{*,\mathrm{aq}} + K_P C_A^2)} \tag{32}$$

$$R_{\mathrm{VII}} = \frac{k_{72} C_A^2 + k_{73} C_A}{(1 + K_H \cdot C_H^{*,\mathrm{aq}} + K_{B2} \cdot C_{B2}^{*,\mathrm{aq}} + K_{B3} \cdot C_{B3}^{*,\mathrm{aq}} + K_P C_A^2)}. \tag{33}$$

The set of rate equations (Eqs. 27–33) encompasses all kinetic expressions given in the literature for these reactions. For example, Corma et al. (1996) proposed a kinetic expression for the oxidation of alcohols by aqueous H_2O_2 over Ti-beta. In their experimental conditions, however, very high concentrations of solvent are implicated, presumably in order to reach a monophasic reaction medium. Thus the solvent adsorption appears in their adsorption term. Moreover, the H_2O_2 concentration C_A is necessarily very low, so that the C_A^2 becomes negligible in the expression of the rate of alcohol oxidation (R_{II} or R_{V}), namely: $k_{22} C_A^2 \ll k_{23} C_A$. Also, in these conditions $C_B^{*,\mathrm{aq}} = C_B$, and the rate becomes:

$$R_{\mathrm{II}} = \frac{k_{21} k_{23} K_B C_B C_A}{1 + K_B C_B},$$

which is essentially the equation of Corma et al. in the absence of a solvent. Very similar expressions of the alcohol oxidation rate on TS-1 were found in the work of Maspero and Romano (1994), in which very low H_2O_2 concentrations were also used as oxidant. Van der Pol and van Hoof (1993) have used similar reaction conditions and a first order of H_2O_2 concentration was also observed in 2-octanol oxidation over TS-1 catalyst. In our articles (Gallot et al., 1996, 1997), the rate of *n*-hexane oxyfunctionalization by aqueous H_2O_2 over TS-1 and TS-2 catalysts was found to fit the following expression:

$$r = \frac{k_1 C_H C_A^2}{1 + K_H + K_B C_B + K_D C_D} \tag{34}$$

In the preceding equations (Eqs. 27–33), this rate would be expressed as

$$r = R_{\mathrm{I}} + R_{\mathrm{III}} + R_{\mathrm{IV}} + R_{\mathrm{VI}}.$$

Obviously this essentially leads to Eq. 34 whenever the square terms are preponderant and, for example, $k_{22} C_A^2 \gg k_{23} C_A$. This condition is more likely to be fulfilled in two liquid-phase systems. It is also clear that in the same conditions, Eqs. 28 and 31 yield essentially Eq. 17, which has been shown to correctly fit the experimental data for 2- and 3-hexanols oxidation reported earlier.

Direct Pathway to Hexanones. In the set of reactions I–VII, it was assumed that 2- and 3-hexanones can be produced by the primary oxidation of *n*-hexane (reactions III and VI). This proposition came from a comparison between the rate constants derived in the present work for the rate of 2- and 3-hexanol oxidation, and the values of these constants obtained in the kinetic analysis of data for the partial oxidation of *n*-hexane on TS-1 catalysts (Gallot et al., 1997). In this last case, the hexanols oxidation reactions were considered as secondary reactions. In this analysis, the direct pathway to hexanones was not considered. If such a pathway exists, this would have led to an overestimation of the hexanol oxidation rate. In this section the presence of this direct pathway to hexanones will be established from examples, of *n*-hexane oxyfunctionalization data.

The data chosen for this calculation were from two experiments performed under similar conditions, with TS-1 catalysts having a Ti/(Ti+Si) ratio of 1.9 and 2.4%, respectively. Figures 9 and 10 contain the experimental values for the adimensional concentration of 2- and 3-hexanols and 2- and 3-hexanones as a function of reaction time for the two catalysts. The other conditions for these two experiments were 0.116 mol of *n*-hexane, 0.0443 mol of H_2O_2, a volume of aqueous and organic phase of 11.22 mL and 15.16 mL, respectively (including a mass of 5 g methanol), a TS-1 catalyst weight of 250 mg, and a temperature of 55°C. In these conditions the solubility equilibrium concentration of *n*-hexane in the aqueous phase ($C_H^{*,\mathrm{aq}}$) was calculated to be 1.43×10^{-2} mol/L.

These data were then fitted to a set of rate equations derived from Eqs. 27–33:

$$R_{\mathrm{I}} = \frac{k_1 C_H^{*,\mathrm{aq}} C_A^2}{Den} \tag{35}$$

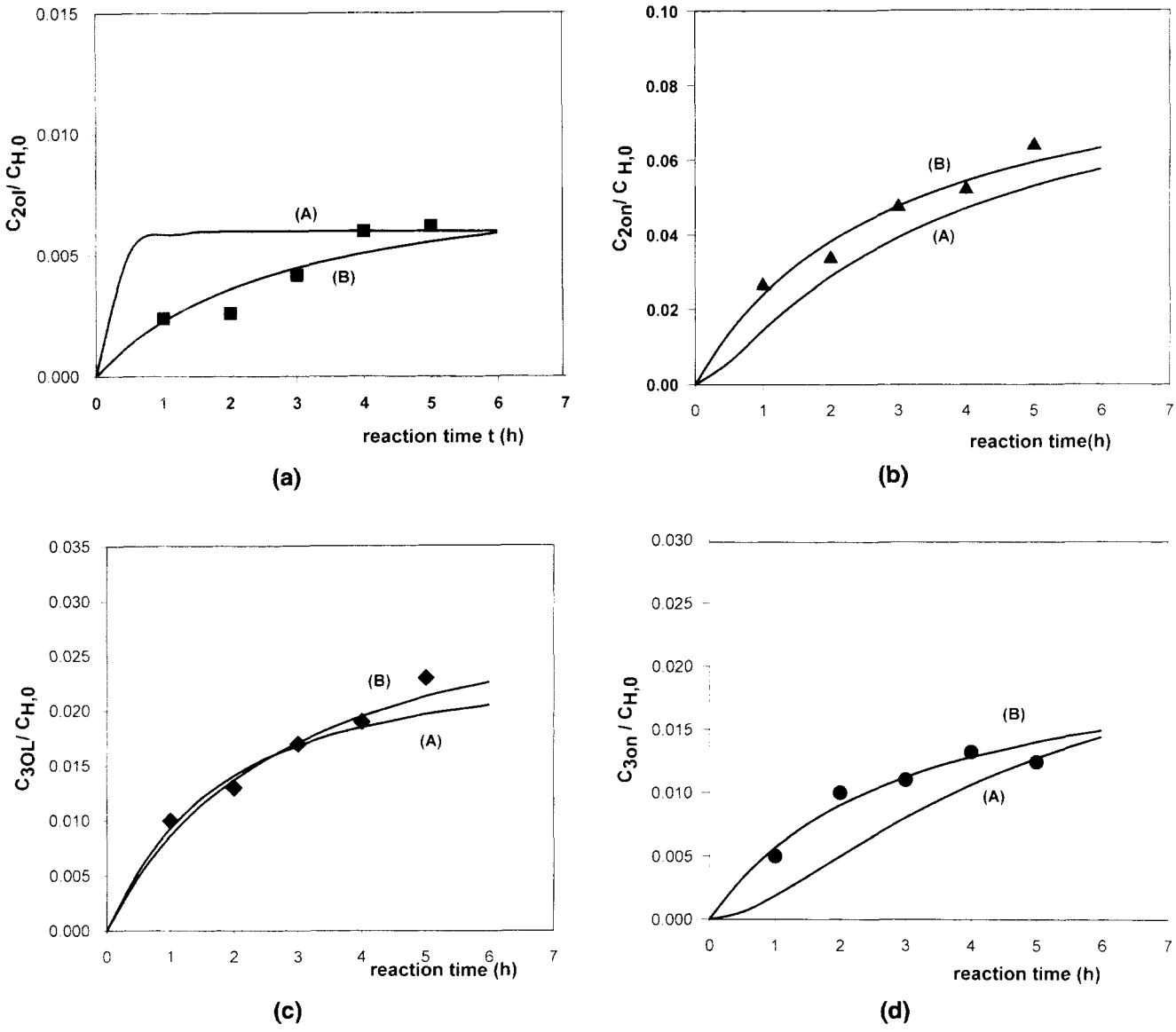

Figure 9. Measured (symbols) and estimated (lines) oxygenate yields distribution during *n*-hexane oxyfunctionalization reaction: $T = 55°C$; TS-1 1.9%.

Curve (A): consecutive reaction model; Curve (B): parallel/consecutive reaction model. (a) 2-Hexanol; (b) 2-hexanone; (c) 3-hexanol; (d) 3-hexanone.

$$R_{II} = \frac{k_{II} C_{B2}^{*,aq} C_A^2}{Den} \tag{36}$$

$$R_{III} = \frac{k_{III} C_H^{*,aq} C_A^2}{Den} \tag{37}$$

$$R_{IV} = \frac{k_{IV} C_H^{*,aq} C_A^2}{Den} \tag{38}$$

$$R_{V} = \frac{k_{V} C_{B3}^{*,aq} C_A^2}{Den} \tag{39}$$

$$R_{VI} = \frac{k_{VI} C_H^{*,aq} C_A^2}{Den} \tag{40}$$

$$R_{VII} = \frac{k_{VII} C_A^2}{Den}, \tag{41}$$

with

$$Den = 1 + K_H C_H^{*,aq} + K_{B2} C_{B2}^{*,aq} + K_{B2} C_{B3}^{*,aq}.$$

Equations 35–41 were thus derived under such assumptions as $k_{22} C_A^2 \gg k_{23} C_A$ and by neglecting $K_P C_A^2$ in the adsorption term.

Assuming a pseudo-steady-state hypothesis and considering that there is no accumulation of organic compounds in the aqueous phase (Gallot et al., 1997), the mass balances of 2- and 3-hexanols (respectively, B_2 and B_3), 2- and 3-hexanones (D_2 and D_3), and hydrogen peroxide were described by the following ordinary differential equations:

$$\frac{d\Psi_n}{dt} = \varsigma \cdot R_n \qquad (n = B_2, D_2, B_3, D_3) \tag{42–45}$$

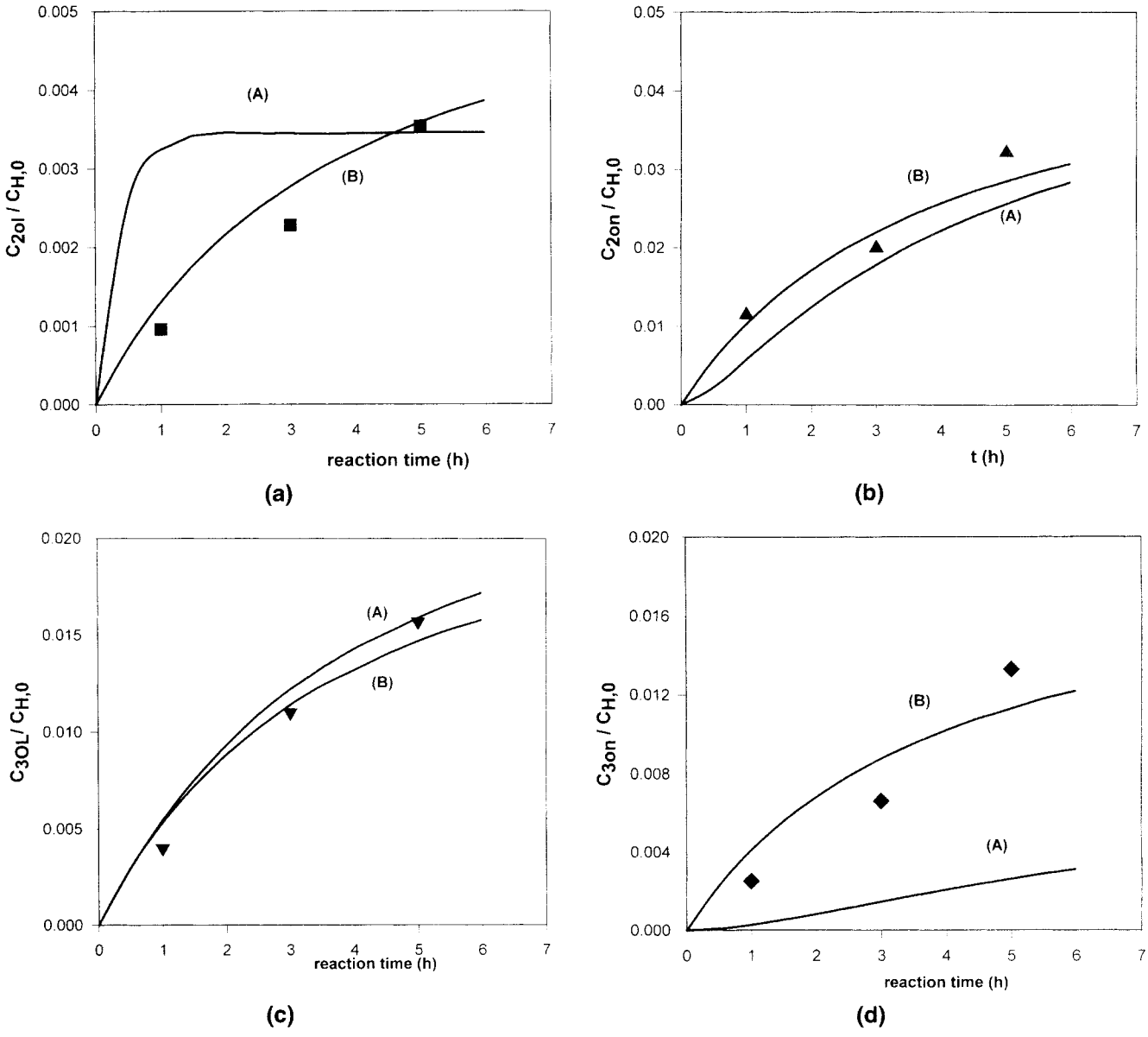

Figure 10. Measured (symbols) and estimated (lines) oxygenate yields distribution during *n*-hexane oxyfunctionalization reaction: $T = 55°C$, TS-1 2.4%.

Curve (A): consecutive reaction model; Curve (B): parallel/consecutive reaction model. (a) 2-hexanol; (b) 2-hexanone; (c) 3-hexanol; (d) 3-hexanone.

$$\frac{d\Psi_A}{dt} = -\sigma \cdot R_A \qquad (46)$$

with

$$\Psi_n = C_n^{\text{org}}/C_{H,0}^{\text{org}} \quad \text{and} \quad \Psi_A = C_A/C_{A,0}, \quad K_i^* = C_i^{*,\text{aq}}/C_i^{*,\text{org}}$$
$$\varsigma = W\text{cat}/N_{H0}, \qquad \sigma = W\text{cat}/N_{A0}.$$

Ψ_n is the oxygenate product yield and Ψ_A is related to the unconverted hydrogen peroxide concentration.

The rates R_n and R_A in Eqs. 42–46 are related to the individual rates R_{I} to R_{VII} in Eqs. 35–41 by

$$R_{B2} = R_{\text{I}} - R_{\text{II}}, \qquad R_{D2} = R_{\text{II}} + R_{\text{III}}$$
$$R_{B3} = R_{\text{IV}} - R_{\text{V}}, \qquad R_{D3} = R_{\text{V}} + R_{\text{VI}}$$
$$R_A = R_{\text{I}} + R_{\text{II}} + R_{\text{IV}} + R_{\text{V}} + R_{\text{VII}} + 2(R_{\text{III}} + R_{\text{VI}}).$$

The set of differential equations (Eqs. 42–46) was solved numerically with the initial reaction condition $[\psi_{B2}, \psi_{D2}, \psi_{B3}, \psi_{D3}, \psi_A]^T = [0, 0, 0, 0, 1]^T$ by Gear's BDF method (IMSL, 1995). The associated rate constants k_{I} to k_{VII} may be estimated by means of the Gauss–Newton–Marquardt method (IMSL, 1995) using data reported in Figures 9 and 10 and the unconverted H_2O_2 concentration evolution with time in the same experiments. These calculations were performed under two hypotheses:

Table 6. Estimated Rate Constants

(a) *n*-Hexane Oxyfunctionalization

Kinetic Parameters ($m^9 \cdot kmol^{-2} \cdot kg^{-1} \cdot h^{-1}$)	Hypothesis A		Hypothesis B	
	TS-1: 1.9%	TS-1: 2.4%	TS-1: 1.9%	TS-1: 2.4%
k_{I}	1.426	0.563	1.16×10^{-1}	6.34×10^{-2}
k_{II}	0.385	0.268	2.68×10^{-3}	5.24×10^{-4}
k_{III}	—	—	0.444	0.255
k_{IV}	0.713	0.286	1.236	0.495
k_{V}	4.91×10^{-2}	1.31×10^{-2}	7.4×10^{-3}	3.1×10^{-3}
k_{VI}	—	—	0.290	0.196
k_{VII} ($m^6 \cdot kmol^{-1} \cdot kg^{-1} \cdot h^{-1}$)	7.18×10^{-2}	5.33×10^{-2}	7.21×10^{-2}	5.32×10^{-2}

(b) 2-,3-Hexanols Oxidation

Kinetic Parameters in Eq. 17 ($m^9 \cdot kmol^{-2} \cdot kg^{-1} \cdot h^{-1}$)	2-,3-Hexanols Oxidation	
	TS-1: 1.9%	TS-1: 2.4%
$k_{1,2}K_{B2}$	2.68×10^{-3}	5.24×10^{-4}
$k_{1,3}K_{B3}$	7.4×10^{-3}	3.1×10^{-3}

($K_{II} = 1.2\times10^{3}$ $m^3 \cdot kmol^{-1}$; $K_{B2} = 0.598$ $m^3 \cdot kmol^{-1}$; $K_{B3} = 0.754$ $m^3 \cdot kmol^{-1}$).

Hypothesis A. Absence of a direct pathway to hexanones. This is simply set as $k_{III} = k_{VI} = 0$ or $R_{III} = R_{VI} = 0$.

Hypothesis B. Presence of a direct path to hexanones ($k_{III} \neq 0$ and $k_{VI} \neq 0$).

For Hypothesis A, the values estimated for the five nonzero rate constants are reported in Table 6, and the corresponding calculated oxygenate yields are given as curves A in Figures 9 and 10. This fit is essentially poor, and the predicted zero hexanone initial selectivities (at time 0) were never observed experimentally. Moreover, constants k_{II} and k_{V}, which correspond to the rates of hexanols oxidation, should be the same as constants k_{12} K_{B2} and k_{13} K_{B3} in Eq. 17. These two constants were estimated from Eq. 19 using the parameter values given in Table 4c and correcting for Ti content using the proportionality relations given in Figure 8 (and corresponding data for 2-hexanol not shown here). Thus, the values estimated from hexanol oxidation experiments are reported in Table 6b. It is clear from the comparison of Table 6a (Hypothesis A) and 6b that $k_{II} > k_{12}K_{B2}$ and $k_{V} > k_{13}K_{B3}$. Thus Hypothesis A is not valid and a direct pathway to hexanones must indeed exist.

Under Hypothesis B, the Gauss–Newton–Marquardt procedure was repeated by setting the k_{II} and k_{V} values to $k_{II} = k_{12}K_{B2}$ and $k_{V} = k_{13}K_{B3}$. In these conditions, the nonzero values reported in Table 6a (Hypothesis B) for k_{III} and k_{VI} were obtained, and this new set of constants was used to derive the curves reported as B in Figures 9 and 10. It is clear that the fit observed in this case is much better than under Hypothesis A. All selectivities (2-/3- and OL/ONE) are correctly predicted as a function of time. Moreover, the initial selectivity to ketone is not predicted to be zero, which corresponds to experimental observations in *n*-hexane oxyfunctionalization. There is therefore little doubt that a direct reaction pathway leading to hexanone occurs during *n*-hexane oxyfunctionalization by H_2O_2 over TS-1.

Conclusions

The kinetic analysis of separate experiments in which 2- and 3-hexanols have been oxydehydrogenated to 2- and 3-hexanones by hydrogen peroxide over TS-1 catalysts allows us to make the following conclusions.

At high H_2O_2 concentrations these reactions are second order with respect to H_2O_2 and first order with respect to the alcohols as described by Eq. 17. This equation was derived in the framework of linear graph theory, assuming that the generation of the surface titanium hydroperoxo intermediate is rate controlling. The two adjustable parameters (k_{1i} and K_{Bi} in Eq. 17) yield estimates with a remarkable internal coherence. They indicate that 2-hexanol is more strongly adsorbed than 3-hexanol (higher $-\Delta H_a$ and $-\Delta S_a$), but the basic kinetic constant $k_{1,i} = k_{1,i}^{app}/K_{Bi}$ is essentially identical with the same activation energy for the two hexanols.

Comparing the preceding results with those of the kinetic analysis performed previously for the oxyfunctionalization of *n*-hexane by H_2O_2 over the same TS-1 samples, it is found that the rate of hexanones production is much lower when hexanol is the primary reactant rather than a product of *n*-hexane conversion. This indicates that hexanone is also produced by a direct primary reaction from *n*-hexane oxidation, parallel to the secondary conversion of produced hexanol.

Introducing this direct pathway to hexanone in the reaction scheme and using graph theory, it was possible to develop Eqs. 35–41. These equations allow a complete representation of the time evolution of all reactants and products involved in the reaction of *n*-hexane oxyfunctionalization. All these conversions and selectivities may now be described as functions of time.

Acknowledgment

Financial support by NSERC through a strategic grant is gratefully acknowledged. The authors also gratefully acknowledge Dr. Do Trong On for catalyst synthesis.

Notation

A, B_k, D_k, H = symbols used, respectively, for H_2O_2, 2- (3) hexanol, 2- (3) hexanone, and *n*-hexane ($k = 2, 3$)
C_i^{org} = organic-phase concentration of component (i), kmol/m^3
C_i = aqueous-phase concentration of component (i), kmol/m^3
N_i = mole number of component (i), mol
(S_k) = catalyst active center
(T_k) = surface intermediate
S = selectivity use of H_2O_2
V^{aq} = aqueous phase volume, m^3
V^{org} = organic phase volume, m^3
Wcat = catalyst weight, kg
α, β, γ = position of H, C atoms or OH group
σ = ratio of catalyst weight to initial mol of *n*-hexane, kg/kmol
ς = ratio of catalyst weight to initial mol of H_2O_2, kg/kmol
ψ = a dimensionless concentration, reduced kinetic parameter
ν = stoichiometric coefficient
φ = reduced kinetic parameter

Literature Cited

Behrens, P., J. Felsche, S. Vetter, G. Schulz-Ekloff, N. I. Jaeger, and W. Niemann, "A XANES and EXAFS Investigation of Titanium Silicalite," *J. Chem. Soc., Chem. Commun.*, 678 (1991).

Bellussi, G., A. Carati, M. G. Clerici, G. Maddinelli, and R. Millini, "Reaction of Titanium Silicalite with Protic Molecules and Hydrogen Peroxide," *J. Catal.*, **133**, 220 (1992).
Boccuti, M. R., K. M. Rao, A. Zecchina, G. Leofanti, and G. Petrini, "Spectroscopic Characterization of Silicalite and Titanium Silicalites," *Stud. Surf. Sci. Catal.*, **48**, 133 (1989).
Cartier, C., C. Lortie, D. Trong On, H. Dexpert, and L. Bonneviot, "Multiple Scattering in Ti K-Edge EXAFS of Siloxytitanium Compound and of Ti Silicalite Catalyst," *Physica B*, **208**, 635 (1995).
Clerici, M. G., G. Bellussi, and U. Romano, "Synthesis of Propylene Oxide from Propylene and Hydrogen Peroxide Catalyzed by Titanium Silicalite," *J. Catal.*, **129**, 159 (1991).
Clerici, M. G., "Oxidation of Saturated Hydrocarbons with Hydrogen Peroxide Catalyzed by Titanium Silicalite," *Appl. Catal. A: Gen.*, **68**, 249 (1991).
Corma, A., P. Esteve, and A. Martínez, "Kinetics of the Oxidation of Alcohols by Hydrogen Peroxide on Ti-Beta Zeolite: The Influence of Alcohol Structure on Catalyst Reactivity," *Appl. Catal. A: Gen.*, **143**, 87 (1996).
Deo, G., A. M. Turek, I. E. Wachs, D. R. C. Huybrechts, and P. A. Jacobs, "Characterization of Titania Silicalite," *Zeolites*, **13**, 365 (1993).
Esposito, A., M. Taramasso, C. Neri, and F. Buonomo, UK Patent 2,116,974 (1985).
Fredunsland, A., R. L. Jones, and J. M. Prausnitz, "Group-Contribution Estimation of Activity Coefficients in Nonideal Liquid Mixtures," *AIChE J.*, **21**, 1086 (1975).
Fu, H., and S. Kaliaguine, "A Kinetic Investigation of Co-Solvent Effects in Oxyfunctionalization of *n*-Hexane by Hydrogen Peroxide on TS-2," *J. Catal.*, **148**, 540 (1994).
Gallot, J. E., H. Fu, M. P. Kapoor, and S. Kaliaguine, "Kinetic Modeling of *n*-Hexane Oxyfunctionalization by Hydrogen Peroxide over Titanium Silicalites of MEL Structure (TS-2)," *J. Catal.*, **161**, 798 (1996).
Gallot, J. E., D. Trong On, M. P. Kapoor, and S. Kaliaguine, "Kinetic of *n*-Hexane Oxyfunctionalization over TS-1: Effect of Ti Content," *Ind. Eng. Chem. J.*, **36**, 3458 (1997).
Geobaldo, F., S. Bordiga, A. Zecchina, and A. Giamello, "DRS UV-vis. and EPR Spectroscopy of Hydroperoxo and Superoxo Complexes in Titanium Silicalites," *Catal. Lett.*, **16**, 109 (1992).
Huybrechts, D. R. C., L. De Bruyker, and P. A. Jacobs, "Oxyfunctionalization of Alkanes with Hydrogen Peroxide on Titanium Silicalites," *Nature*, **345**, 242 (1990).
Huybrechts, D. R. C., I. Vaesen, H. X. Li, and P. A. Jacobs, "Factors Influencing the Catalytic Activity of Titanium Silicalites in Selective Oxidation," *Catal. Lett.*, **8**, 237 (1991).
Huybrechts, D. R. C., P. Buskens, and P. A. Jacobs, "Physicochemical and Catalytic Properties of Titanium Silicalites," *J. Mol. Catal.*, **71**, 129 (1992).
IMSL Mathematical Software Library (1995).
Le Noc, L., C. Cartier dit Moulin, S. Solomykina, D. Trong On, C. Lortie, S. Lessard, and L. Bonneviot, *Proc. Int. Zeol. Symp., Quebec, Stud. Surf. Sci. Catal.*, **97**, 19 (1995).
Maspero, F., and U. Romano, "Oxidation of Alcohols with H_2O_2 Catalyzed by Titanium Silicalites," *J. Catal.*, **146**, 476 (1994).
Millini, R., E. Previde Massara, G. Perego, and G. Bellussi, "Framework Composition of Titanium Silicalite-1," *J. Catal.*, **137**, 497 (1992).
Perego, G., G. Bellussi, C. Corno, M. Taramasso, F. Buonomo, and A. Esposito, *Stud. Surf. Sci. Catal.*, **28**, 129 (1986).
Pritchard, D. J., and D. W. Bacon, "Prospects for Reducing Correlations Among Parameter Estimates in Kinetic Models," *Chem. Eng. Sci.*, **33**, 1539 (1978).
Roffia, P., and M. Padovan, Eur. Patent 0,208,311 A2 (1987).
Seinfeld, J. H., and L. Lapidus, *Mathematical Method in Chemical Engineering*, Vol. 3, *Process Modeling, Estimation and Identification*, Prentice Hall, Englewood Cliffs, NJ (1978).
Tatsumi, T., M. Nakamura, S. Negeshi, and H. Tominaga, "Shape-Selective Oxidation of Alkanes with H_2O_2 Catalyzed by Titanosilicate," *J. Chem. Soc., Chem. Commun.*, **476** (1990).
Trong On, D., L. Bonneviot, A. Bittar, A. Sayari, and S. Kaliaguine, "Titanium Sites in Titanium Silicalite: A XPS, XANES, and EXAFS Study," *J. Mol. Catal.*, **74**, 233 (1992a).
Trong On, D., A. Bittar, A. Sayari, S. Kaliaguine, and L. Bonneviot, "Novel Titanium Sites in Silicalites,'" *Catal. Lett.*, **16**, 85 (1992b).
Tuel, A., J. Diab, P. Gelin, M. Dufaux, J. F. Dutel, and Y. Ben Taârit, "EPR Evidence for the Isomorphous Substitutions of Titanium in Silicalite Structure," *J. Mol. Catal.*, **63**, 95 (1990).
Uguina, M. A., D. P. Serrano, G. Ovejero, R. Van Grieken, and M. Camacho, "Preparation Of TS-1 by Wetness Impregnation of Amorphous SiO_2-TiO_2: Influence of Synthesis Variable," *Appl. Catal. A: Gen.*, **124**, 391 (1995).
Van der Pol, A. J. H. P., and J. H. C. van Hoof, "Oxidation of Linear Alcohols with Hydrogen Peroxide over Titanium Silicalite-1," *Appl. Catal. A: Gen.*, **106**, 97 (1993).
Yablonskii, G., Bykov, V., Gorban, A., and Elokhin, V., *Comprehensive Chemical Kinetics*, Vol. 32, *Kinetic Models of Catalytic Reactions*, R. G. Compton, ed., Elsevier, Amsterdam (1991).
Zecchina, A., G. Spoto, S. Bordigas, A. Ferrero, G. Petrini, G. Leofanti, and G. Padovan, "Framework and Extraframework Ti in Titanium-Silicalite: Investigation by Means of Physical Method," *Zeolite Chemistry and Catalysis*, Elsevier, Amsterdam (1991).

Manuscript received Sept. 12, 1997, and revision received Mar. 10, 1998.